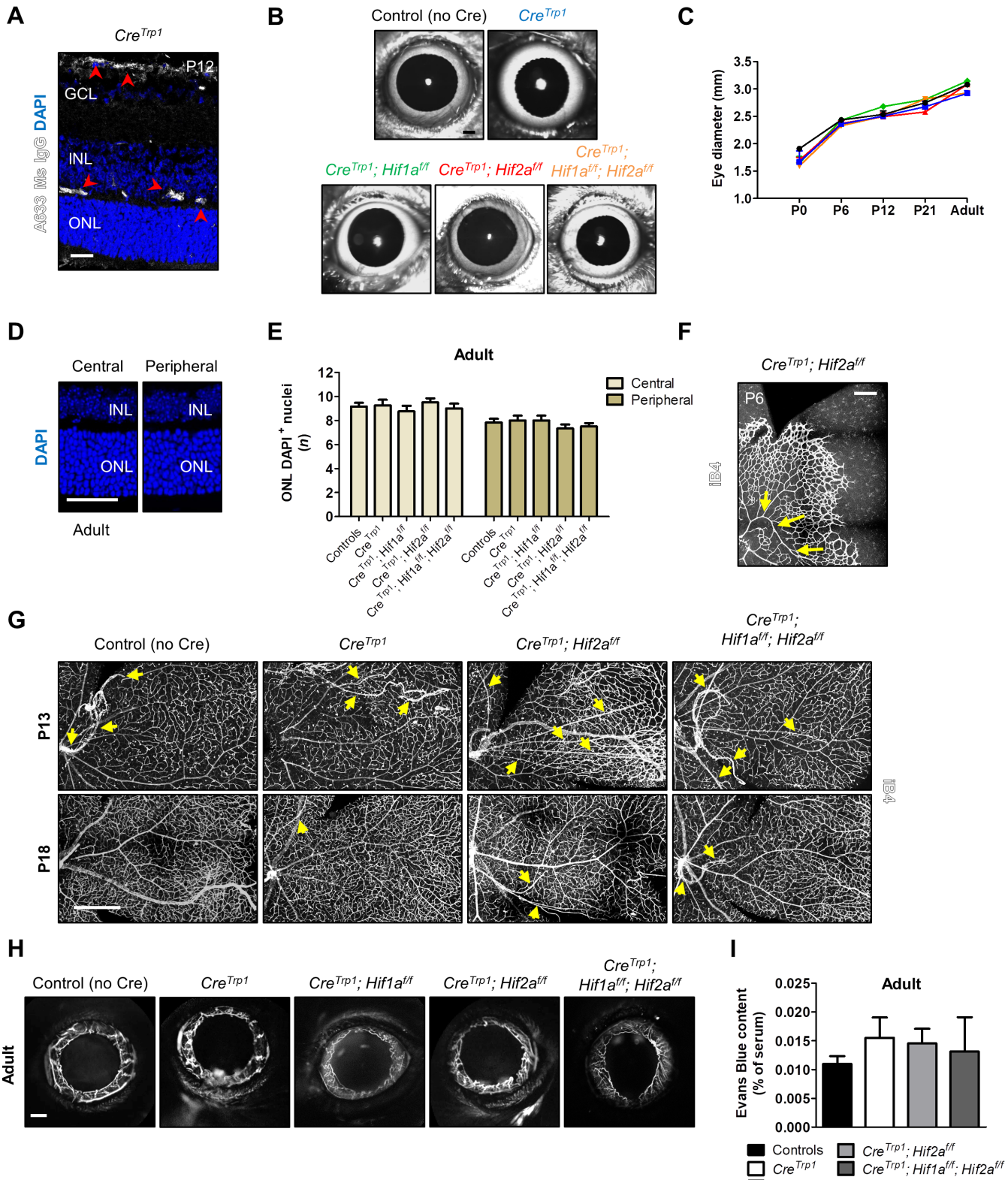

Fig. S1. Deletion of *Hif2a* does not result in eye size changes, photoreceptor degeneration, alterations in iridal vasculature, adult vascular severely persistent hyaloid vasculature or permeability increase. (A) Representative secondary antibody only staining control of P12 Cre^{Trp1} eye section. Positive labelling of blood vessels highlighted by red-arrowheads. (B) AF-SLO imaging of representative adult eyes for each genotype analysed. (C) Time-course of post-natal eye growth for the genotypes analysed. Refer to coloured labels in (B). n = 6-12 animals/group. No significant differences observed (ANOVA). (D) Representative images of ONL nuclei in adult eyes and (E) quantification of $DAPI^+$ nuclei rows in the peripheral and central ONL regions (2 pictures/region/animal quantified). n = 4-6 animals/group. No significant differences observed (ANOVA). (F) Representative image of a bended developing artery at P6 of Cre^{Trp1};$Hif2a^{f/f}$ genotype (yellow arrows) on a retinal flatmount stained with iB4. (G) iB4 staining of retinal whole mounts, from which the hyaloid vasculature had not been removed, shows some residuals at P13 (yellow arrows) in all genotypes, and very few at P18 in *Hif2a* KO and Cre^{Trp1} genotypes. (H) ICGA angiography of the outer portion of the eye shows normal anatomy of the iridal vasculature in all genotypes observed. (I) Evans Blue extravasation assay did not show any significant change in retinal permeability (ANOVA) in *Hif2a* KO genotypes compared to controls and Cre^{Trp1}. n = 5-15 animals/group. Scale bars: (A) 25μm (B) 1mm; (D) 50μm; (F) 1mm; (G) 50μm; (H) 25μm.

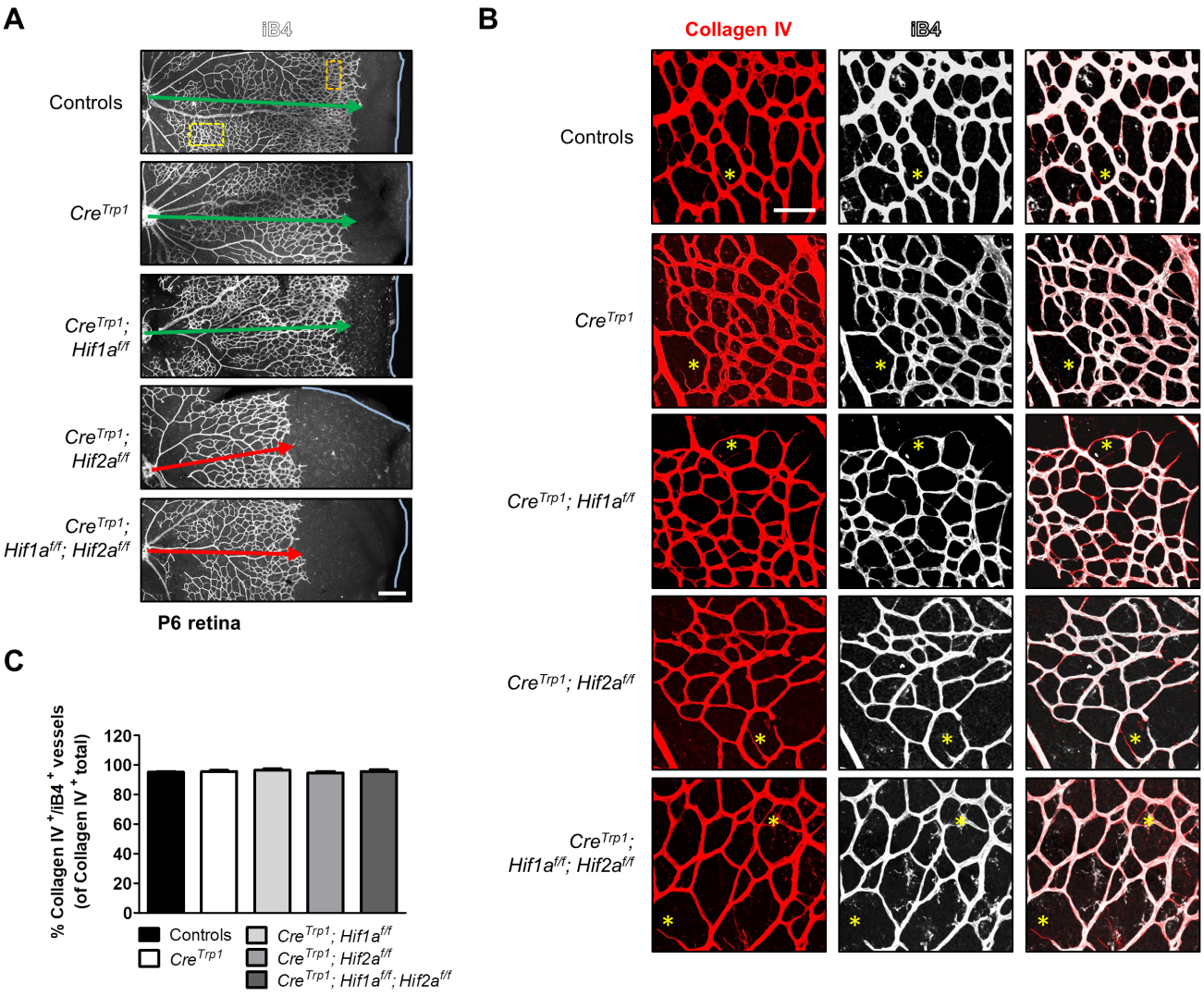

Fig. S2. *Hif2a* deletion does not increase vessel regression. (A) Representative iB4 staining of retinal flatmounts (age: P6) from different genotypes analysed. Orange (angiogenic front) and yellow (capillary bed) boxes in (A) are examples of fields used for branch points quantification in Fig. 3C-D; light blue line indicates the edge of the retina (B) Collagen IV and iB4 staining of P6 retinae. Yellow asterisks show empty Collagen IV sleeves. (C) Quantification of Collagen IV^{+}/iB4^{+} vessels (4 fields/animal measured). Results are from n = 5-6 animals/genotype. No significant differences observed (ANOVA). Scale bars: 250μm (A), 75μm (B).

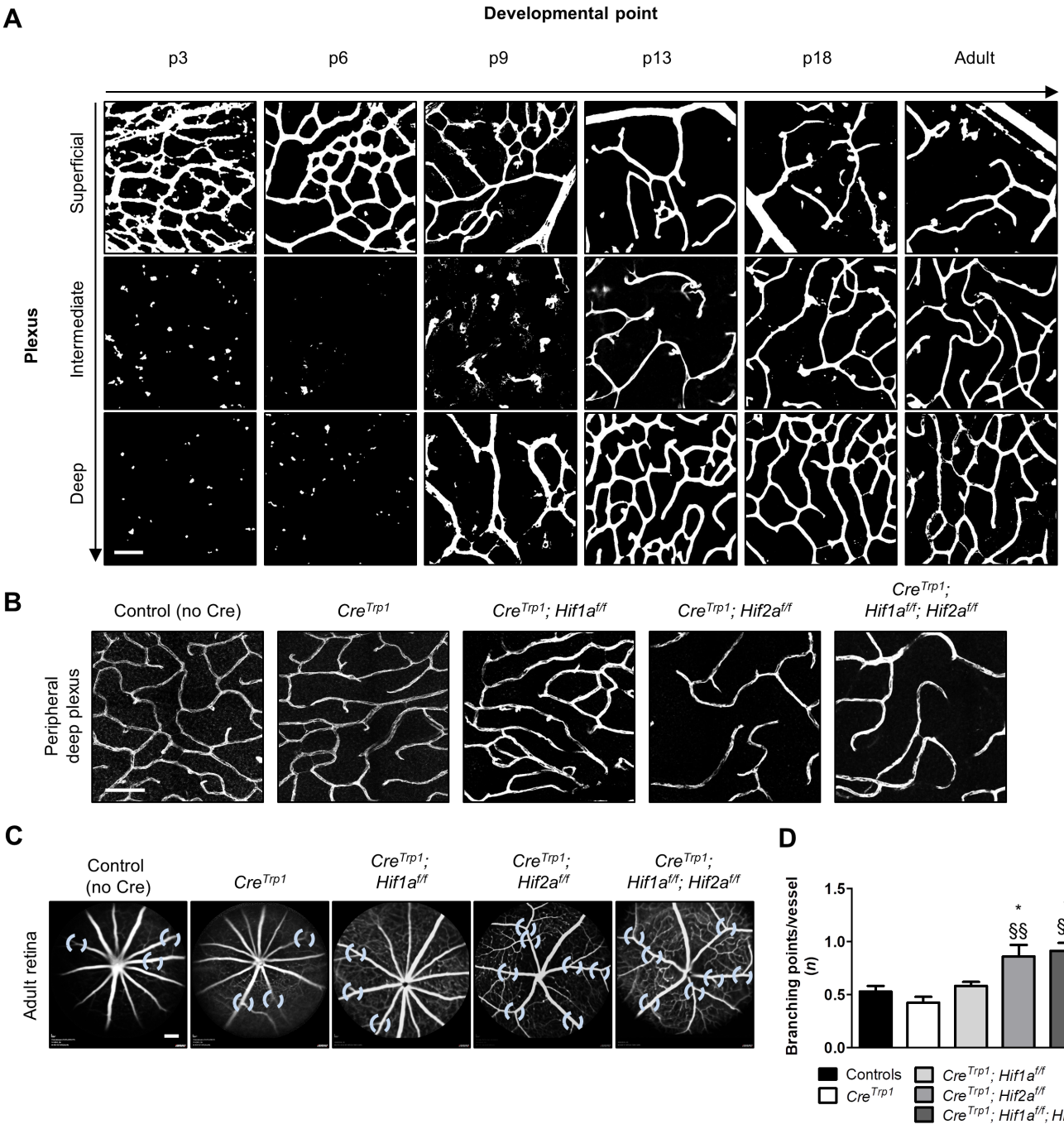

Fig. S3. Wild-type vascular plexi development; peripheral deep plexus abnormalities in adult *Hif2a* KO lines; increased number of major vessels branch points in *Hif2a* KO lines. (A) Representative confocal pictures of iB4 staining of retinal flatmounts, representative of normal central retina plexi development over time (P3 to adulthood). Average density values (n = 5-12 time point) of the controls group were used as reference to calculate vascular development in other genotypes. (B) Representative confocal pictures of adult permanent peripheral deep plexus alterations in *Hif2a* KO lines. (C) Representative AF-SLO pictures of adult animals, showing an increased number of branch points arising from major vessels (light-blue circles). Differences are quantified in (D). n = 7-14 animals/group. ANOVA and Tukey's multiple comparison test results: **P*<0.05 vs. controls; §§*P*<0.05 vs. Cre^{Trp1}. Scale bars: (A) 75µm; (B) 75µm; (C) 1mm.

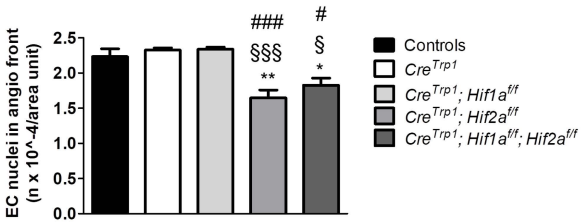

Fig. S4. Decreased number of endothelial cells at the angiogenic front in the developing vasculature of *Hif2a* KO lines. Quantification of endothelial cells nuclei (stained with Erg) at the angiogenic front (representative images in Fig. 4A). n=5 animals/group; 4 fields/animal quantified. ANOVA and Tukey's multiple comparison test results: **P*<0.05, ***P*<0.01 vs. controls; §*P*<0.05, §§§*P*<0.001 vs. *Cre*^{Trp1}; #*P*<0.05, ###*P*<0.001 vs. *Cre*^{Trp1}*;Hif1a*$^{f/f}$.

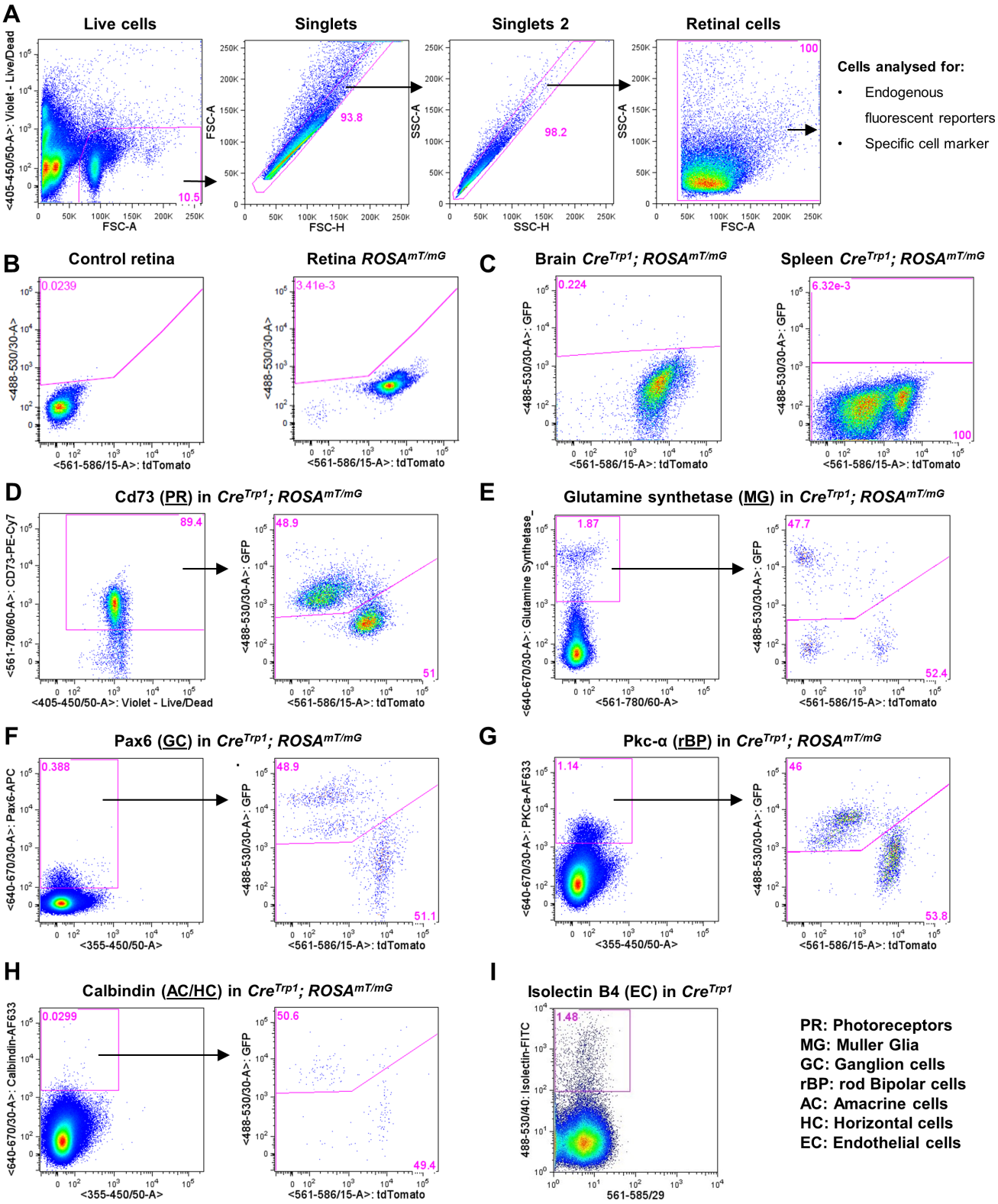

Fig. S5. Example of flow cytometry analysis of cell markers used to characterise the cellular composition of dissociated whole retina. (A) Flow cytometry gating strategy for analysis of dissociated retinal samples. This example shows a young adult (4-6 weeks of age) dissociated retina stained with DraQ7 to exclude dead cells and cellular debris and identify the live cell population, which was then plotted to exclude cellular aggregates and to identify only single cells ("singlets" and "singlets 2"). Relative size (FSC-A) and granularity (SSC-A) of single, live retinal cells is then obtained before proceeding to endogenous fluorescent markers and/or antibody staining detection and analysis. (B) Representative plots of control and *ROSA*$^{mT/mG}$ retinal samples. GFP^{+} gate is comparable to the one used to analyse *Cre*^{Trp1}*;ROSA*$^{mT/mG}$ retinae. (C) Representative plots of *Cre*^{Trp1}*;ROSA*$^{mT/mG}$ brain and spleen samples. (D) Representative plot of CD73 staining on *Cre*^{Trp1}*;ROSA*$^{mT/mG}$ retina, chosen to label photoreceptors, and subsequent GFP/tdTomato analysis on the gated population. (E) Representative plot of glutamine Synthetase (GS^{+}) staining on *Cre*^{Trp1}*;ROSA*$^{mT/mG}$ retina, selected to label Müller Glia, and subsequent GFP/tdTomato analysis on the gated population. (F) Representative plot of Pax6 staining on *Cre*^{Trp1}*;ROSA*$^{mT/mG}$ retina, selected to label ganglion cells, and subsequent GFP/tdTomato analysis on the gated population. (G) Representative plot of Pkc-α staining on *Cre*^{Trp1}*;ROSA*$^{mT/mG}$ retina, selected to label rod bipolar cells, and subsequent GFP/tdTomato analysis on the gated population. (H) Representative plot of Calbindin staining on *Cre*^{Trp1}*;ROSA*$^{mT/mG}$ retina, selected to label amacrine and horizontal cells, and subsequent GFP/tdTomato analysis on the gated population. (I) Representative plot showing live FITC-iB4^{+} cells in a control retinal sample; these cells were sorted into TRIzol plus for further mRNA extraction and transcriptome analysis (Fig. 2J).

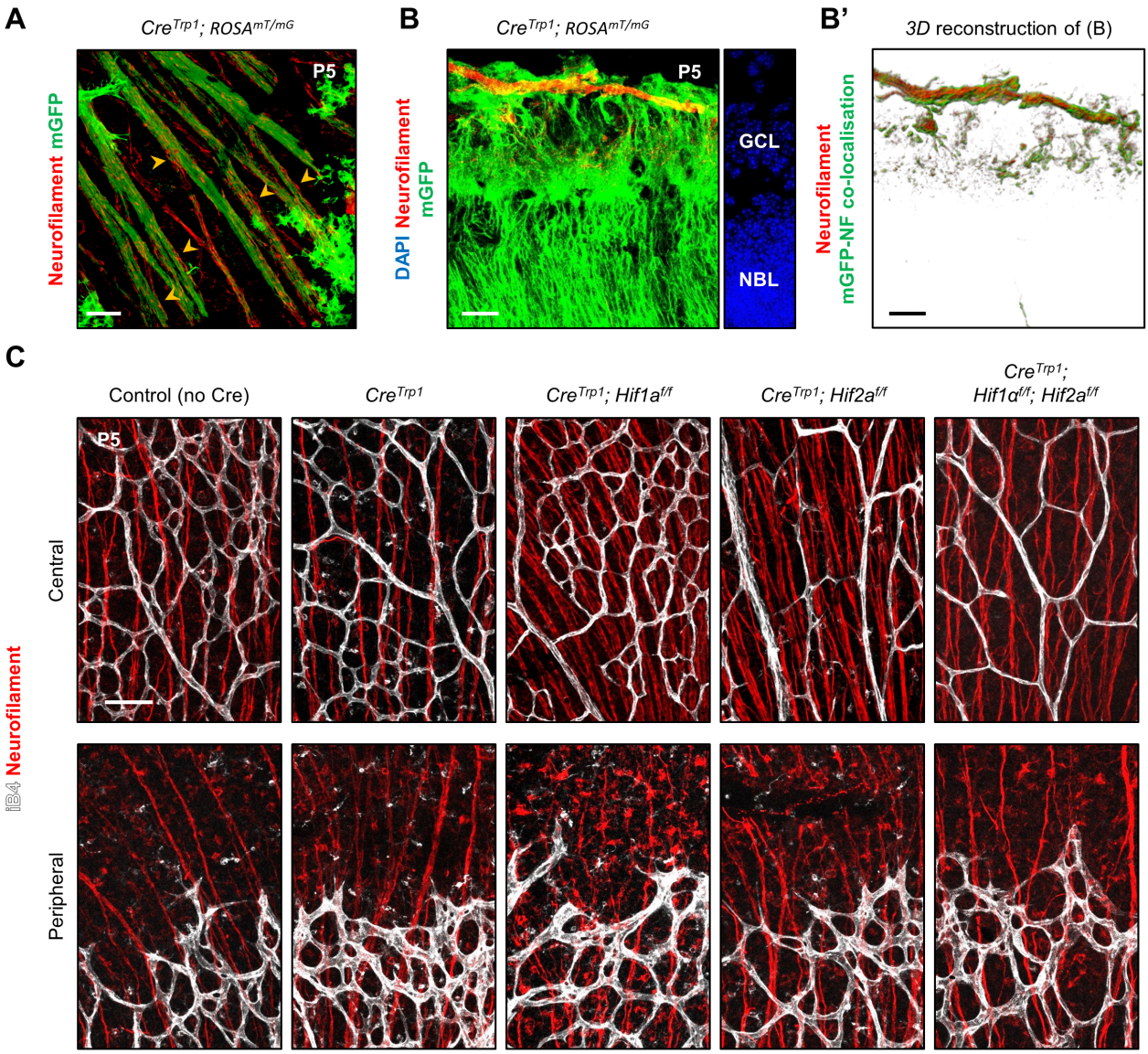

Fig. S6. Ganglion cells axon morphology and spatial organisation are not altered. Confocal images of flatmount (A) and section (B) of P5 *Cre^{Trp1};ROSA$^{mT/mG}$* line showing co-localisation between GFP^{+} cells and retinal ganglion cells marker neurofilament (yellow arrow-heads). (B') Imaris re-construction of (B). (C) Representative confocal images (central retina – mature capillary bed; peripheral – angiogenic front) of immuno-stained ganglion cells and axons, showing normal distribution and morphology in all the genotypes analysed. Scale bars: 25µm (A-B'); 75µm (C).

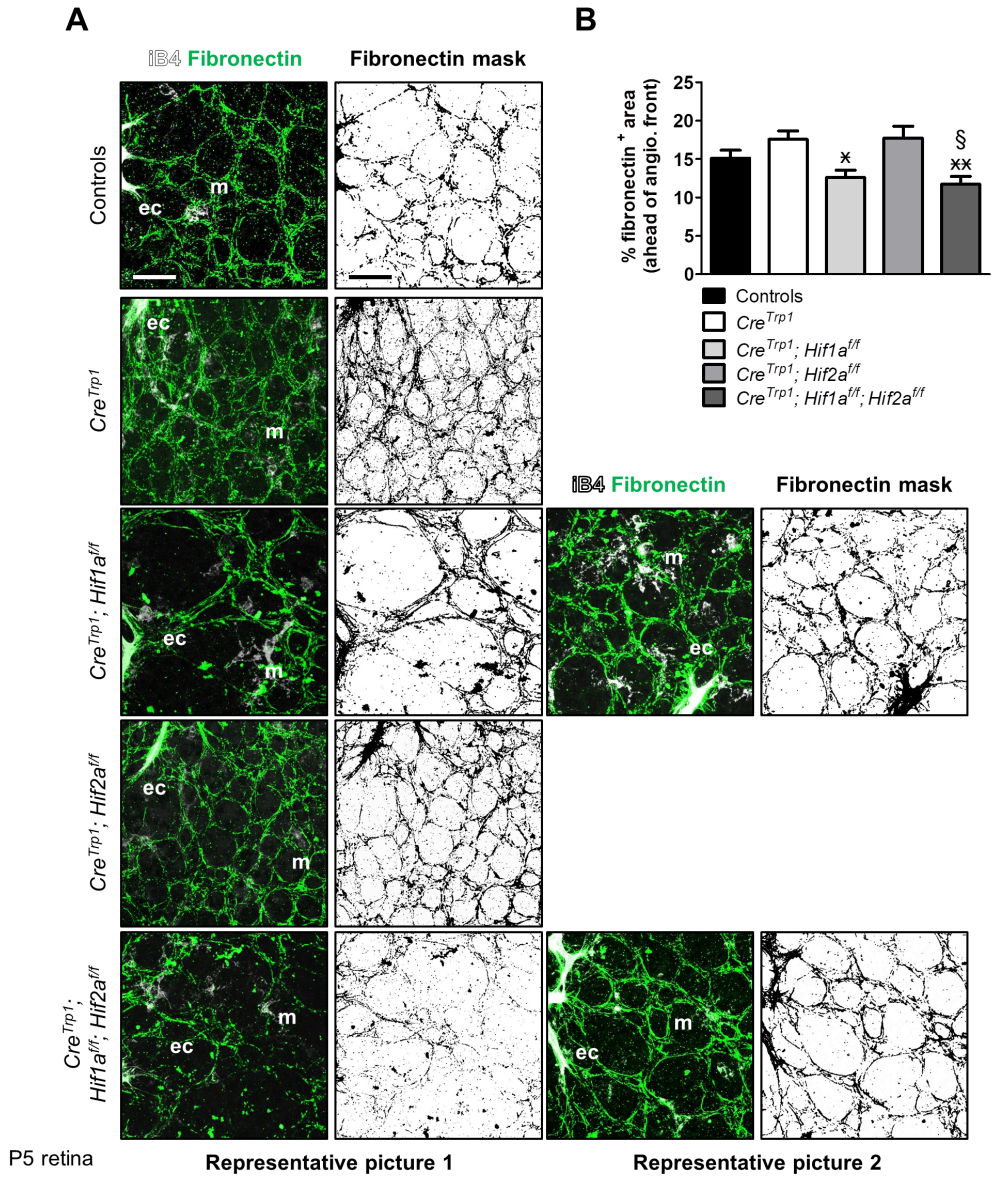

Fig. S7. Astrocyte-mediated fibronectin deposition ahead of the angiogenic front. (A) Representative images of deposited fibronectin ahead of the angiogenic front (age: P5). Significant differences are only evident in *Cre*^{Trp1}*;Hif1a*$^{f/f}$ and *Cre*^{Trp1}*;Hif1a*$^{f/f}$*;Hif2a*$^{f/f}$, although not in every field of view analysed (see representative picture 2). (B) Quantification of area occupied by fibronectin-positive filaments ahead of the angiogenic front (expressed as percentage of total area analysed). n=5-9 animals/genotype; 4 fields of view/animal. ANOVA and Tukey's multiple comparison test results: §P<0.05 vs. *Cre*^{Trp1}; *⁎*P<0.05, *⁎⁎*P<0.01 vs. *Cre*^{Trp1}*;Hif2a*$^{f/f}$. Scale bar: 25µm (A).

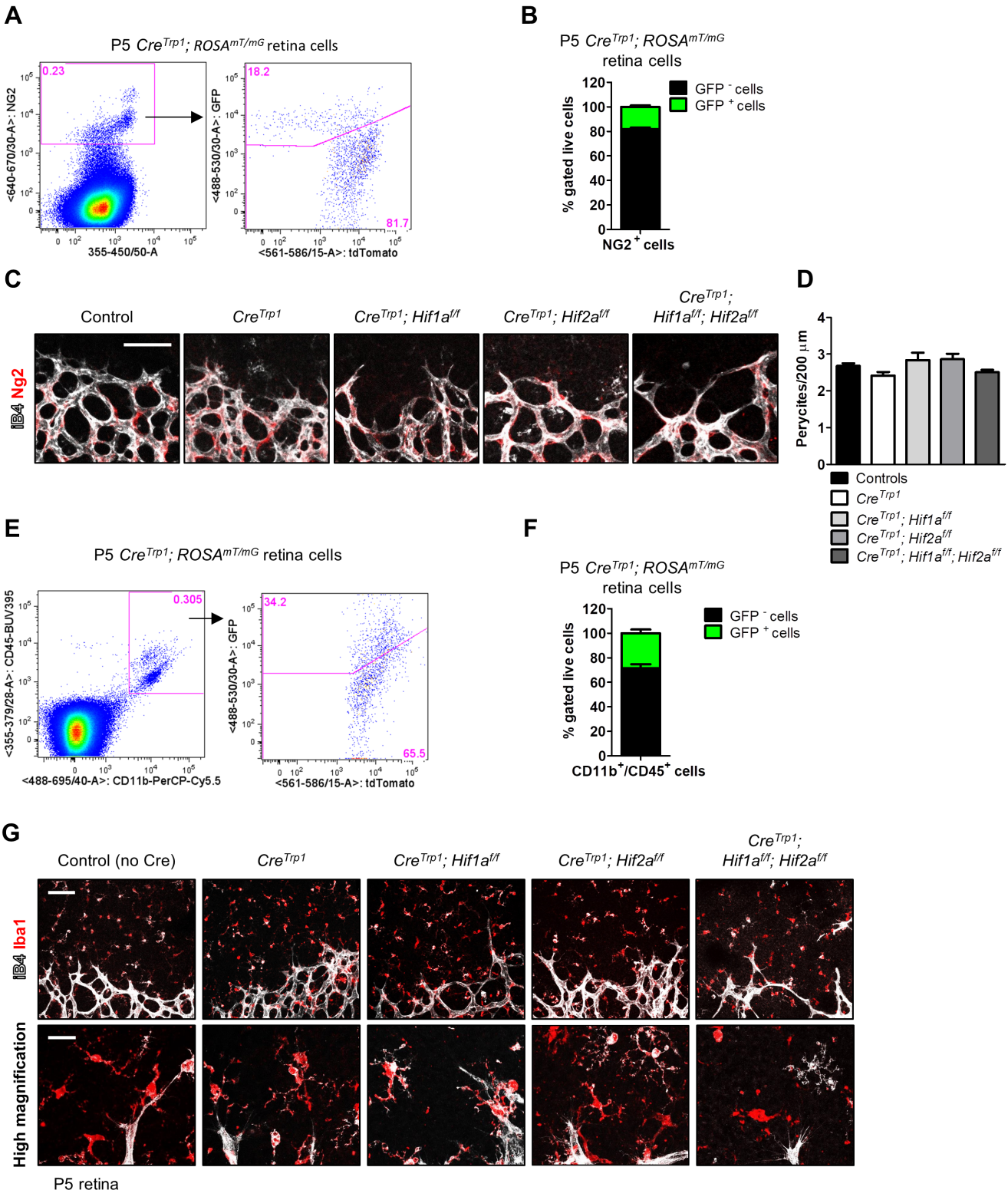

Fig. S8. Pericytes and resident microglia are partially affected by Cre expression in *Cre^{Trp1}* lines but their spatial organisation and morphology at the angiogenic front is unaltered. (A) Representative flow cytometric plot of Ng2/GFP^{+} cells in P5 *Cre^{Trp1};ROSA$^{mT/mG}$*. (B) Quantification of GFP^{+} and GFP^{-} Ng2^{+} cell population. n=5 animals/genotype. (C) Normal distribution of Ng2^{+} pericytes at the angiogenic front (age: P5). (D) Quantification of pericytes density. n=5-6 animals/genotype; 4 fields of view/animal. No significant differences between genotypes (ANOVA). (E) Representative flow cytometric plot of CD11b/CD45/GFP^{+} cells in P5 *Cre^{Trp1};ROSA$^{mT/mG}$*. (F) Quantification of GFP^{+} and GFP^{-} CD11b/CD45^{+} cell population. n=5 animals. (G) Representative images at the angiogenic front showing normal presence of Iba1^{+} resident myeloid cells and higher magnification to appreciate cellular morphology. Scale bar: 75µm (C, G); 25µm (G high magnification).

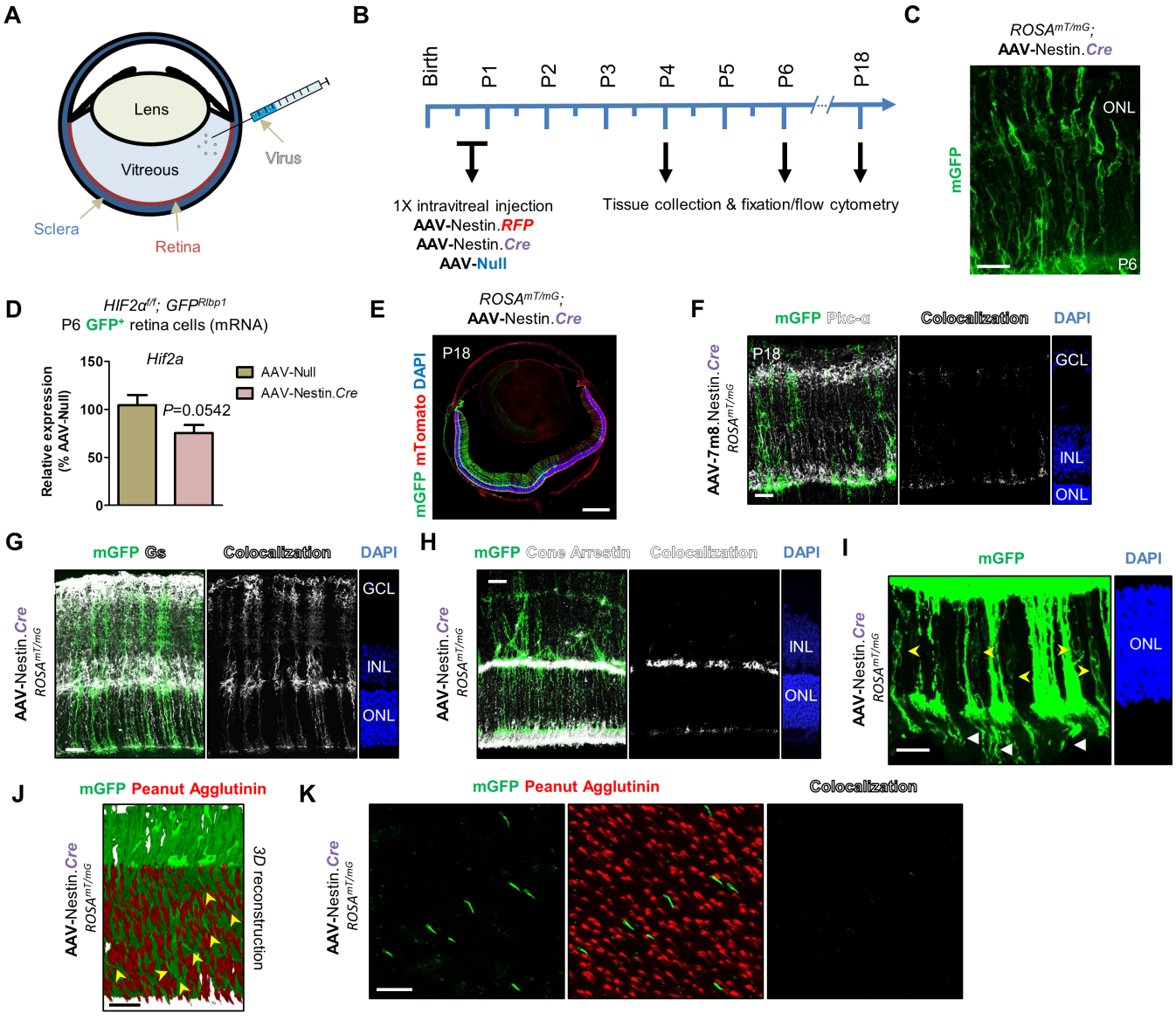

Fig. S9. AAV-Nestin.*Cre* targets late progenitor cells. (A) Schematic describing intravitreal micro-injection. (B) Experimental time-line. For vasculature development experiments, one eye was injected with AAV-Nestin.*Cre*, whereas the controlateral with AAV-Null. (C) Representative image of P6 *ROSA*$^{mT/mG}$ injected with AAV-Nestin.*Cre*. (D) RT-qPCR analysis of *Hif2a* in GFP^{+} cells FACS-sorted from P6 control *Hif2a*$^{f/f}$*;GFP*^{Rlbp1} eyes injected with either AAV-Null or AAV-Nestin.*Cre*. Values are expressed as percentage relative to Null injected and are from n = 7 animals/group. Unpaired *t*-test result indicated. (E) P18 *ROSA*$^{mT/mG}$ eye injected intravitreally with AAV-Nestin.*Cre* virus. Sections were then stained with Pkc-α (F), Glutamine Synthetase (GS) (G) and cone arrestin (H). GFP signal convincingly co-localises with GS^{+} cells (Müller glia), only minimally with Pkc-α, whereas any co-localisation with cone arrestin is produced by random juxtaposition of the two stains. (I) Rod photoreceptor cell bodies are evident in the ONL of a P18 virally-treated *ROSA*$^{mT/mG}$ eye (yellow arrow-heads), as well as the outer segments (white arrow-heads). (J) *3D* reconstruction of a fine *z*-stack acquired from a P18 virally-treated *ROSA*$^{mT/mG}$ retina, showing cells derived from virally-targeted cells (GFP^{+}) and cones outer segments (PNA-stained). (K) *Z*-projection of the outer segments layer shows no co-localization between GFP^{+} segments and cone segments. Scale bars: 25μm (C, F-K); 500μm (E).

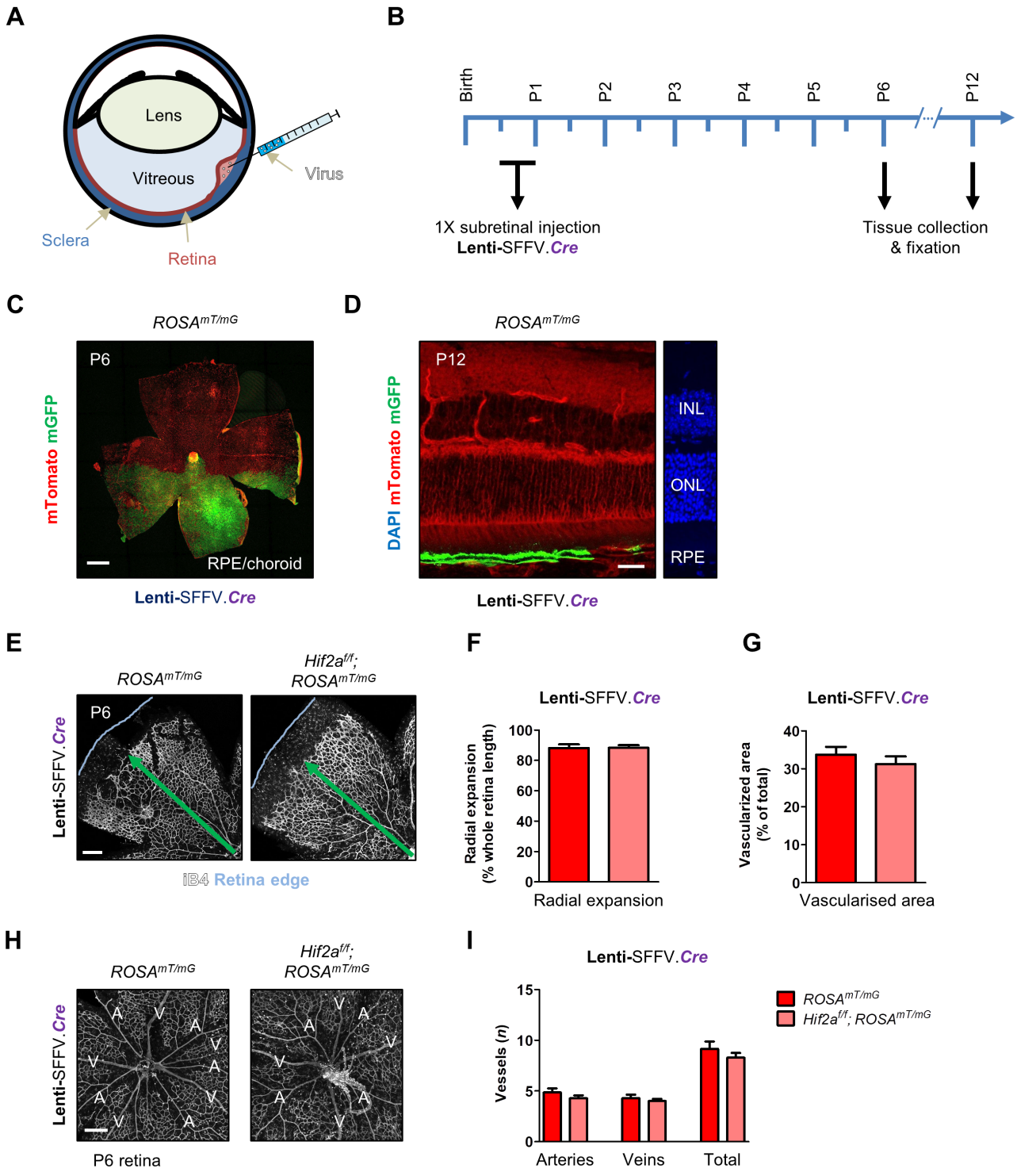

Fig. S10. RPE-targeted delivery of *Cre* recombinase to *Hif2a$^{f/f}$* line does not replicate the vascular phenotype observed in *Cre^{Trp1};Hif2a$^{f/f}$* mice. (A) Schematic describing subretinal micro-injection. (B) Experimental time-line. (C) Representative RPE/choroid flatmount (age: P6; *ROSA$^{mT/mG}$* genotype) showing mGFP^{+} areas targeted by lentiviral-mediated Cre recombinase delivery. (D) Section from an eye injected with Lenti.VSVG.SFFV.*Cre* (age: P12; *ROSA$^{mT/mG}$*). (E) Representative confocal images of iB4-stained P6 retinal flatmounts injected with Lenti.VSVG.SFFV.*Cre* (genotypes: *ROSA$^{mT/mG}$*; *Hif2a$^{f/f}$;ROSA$^{mT/mG}$*). (F) and (G) show quantification of vascular development (age: P6) in terms of radial expansion and vascularised area. Only retinal regions above strongly transduced RPE regions were quantified. n=8 animals/group. No significant differences between groups (unpaired *t*-test). (H) Arteries and veins in virally-injected eyes (age: P6). (I) Big vessels were quantified and compared (by unpaired *t*-test; no difference). Scale bars: 500μm (C); 25μm (D); 250μm (E, H).

Marker(s)	Cell target	Abbreviation	Reference
CD73	Photoreceptors	PR	Koso et al., 2009
Glutamine Synthetase	Müller glia	MG	Grossman et al., 1994
Pkc-a	Rod bipolar cells	rBP	Ruether et al., 2010
Calbindin	Amacrine/ Horizontal cells	AC/HC	Liu et al., 2013
Pax6	Ganglion cells/retinal progenitor cells	GC/RPC	Hitchcock et al., 1996; Stanescu-Segall et al., 2015
PDGFR-a	Astrocytes	A	Tao and Zhang, 2014
CD11b/CD45	Myeloid cells	MC	Liyanage et al., 2016
NG2	Pericytes	P	Ozerdem et al., 2001

Supplemental Table S1: Markers used by flow cytometry for cell type characterisation.

Markers used for immuno-staining of *Cre* ^{Trp1} ; *ROSA* $^{mT/mG}$ neuroretinae are listed and referenced.

Adult retina	% of total *Cre* ^{Trp1} ; *ROSA* $^{mT/mG}$ retina (live events)	% GFP^{+} population in *Cre* ^{Trp1} ; *ROSA* $^{mT/mG}$ retina (live events)	Reference % from (Jeon et al., 1998; Macosko et al., 2015)
Photoreceptors	82.4	81.3	82.1
Müller glia	1.17	1.82	2.80
Rod Bipolar cells	1.54	1.62	* 7.3
Amacrine/horizontals	0.024	0.020	7.00
Ganglion cells	0.45	0.48	0.50
Astrocytes	0.09	0.07	0.10
Myeloid cells	0.28	0.11	0.20
Pericytes	0.20	0.10	ND
Undetermined	13.82	14.49	7.30
Total	100.00	100.00	100.00

Supplemental Table S2: Comparison of cell type percentages to published values.

Values obtained for each retinal cell type (in adult whole Cre^{Trp1}; ROSA$^{mT/mG}$ retina and GFP+ gated population) are compared to reference values reported in the literature (25, 26)

* Value relative to the entire bipolar cells population (as opposed to only rod bipolar cells, identified by PKCa in this study).

Antigene	Antibody species (fluorescent label)	Supplier (catalogue number)	Application	Dilution	Intracellular/extracellular (FC)
Arrestin 3	Rabbit	Novus Biologicals (NBP1-19629)	IF	1:200	
Collagen IV	Rabbit	Bio-Rad (2150-1470)	IF	1:200	
Cre recombinase	Mouse	Millipore (MAB 3120)	IF	1:100	
ERG	Rabbit	Abcam (ab92513)	IF	1:200	
Fibronectin	Rabbit	Millipore (AB 2033)	IF	1:200	
GFAP	Rabbit	Dako (Z0334)	IF	1:200	
Hif2a	Rabbit	Novus Biologicals (NB100)	IF	1:200	
Iba1	Rabbit	Alpha Labs (019-19741)	IF	1:1000	
Isolectin B4 (biotin-conjugated)	N/A	Sigma-Aldrich (L2140)	IF	1:200	
Neurofilament-L	Rabbit	Millipore (C28E10)	IF	1:500	
Beta-Actin	Mouse	R&D Systems (MAB8929)	WB	1:5000	
Beta-Tubulin	Mouse	Sigma-Aldrich (T4026)	WB	1:1000	
Endostatin	Goat	R&D Systems (AF570-SP)	WB	1:1000	
Total VEGFR2	Rabbit	Cell Signalling (9698)	WB	1:1000	
VEGFR2 pY1175	Rabbit	Cell Signalling (3770)	WB	1:1000	
Calbindin	Mouse	Abcam (ab75524)	FC	1:50	Intracellular (fixed)
CD11b	Rat (PerCP-Cy5)	Biolegend (101227)	FC	1:100	Extracellular (unfixed)
CD45	Rat (BUV-395)	BD Biosciences (565967)	FC	1:100	Extracellular (unfixed)
CD73	Rat (PE-Cy7)	Thermo Fisher Scientific (25-0731-80)	FC	1:100	Extracellular (unfixed)
Glutamine synthetase	Mouse	BD Biosciences (610517)	IF/FC	1:200 (IF)/1:50 (FC)	Intracellular (fixed)
Isolectin B4 (FITC-conjugated)	N/A	Vector Labs (FL-1201)	FC	1:100	Extracellular (unfixed)
NG2 Chondroitin Sulfate Proteoglycan	Rabbit	Millipore (AB 5320)	IF/FC	1:200 (IF)/1:50 (FC)	Intracellular (fixed)
Pax6	Rat (APC)	Miltenyi Biotec (130-107-829)	IF/FC	1:100 (IF)/1:50 (FC)	Intracellular (fixed)
PDGFRa	Rat (APC)	Biolegend (APA5)	IF/FC	1:100 (IF)/1:50 (FC)	Extracellular (unfixed)
PKCa	Rabbit	Santa Cruz (H-7)	IF/FC	1:200 (IF)/1:50 (FC)	Intracellular (fixed)

Secondary antibody	Antibody species	Supplier	Application	Dilution
AF633-conjugated secondary antibodies	Goat	Thermo Fisher Scientific (A21052; A21070; S21375)	IF/FC	1:500 (IF)/1:200 (FC)
Biotin-conjugated secondary antibodies	Goat	Thermo Fisher Scientific (31430; 31460)	WB	1:2000 - 1:5000
Biotin-conjugated secondary antibodies	Rabbit	Dako (P0449)	WB	1:2000

Supplemental Table S3: List of antibodies and conditions used.

List of antibodies, dilutions and fixation used for immunofluorescence (IF), western blotting (WB) and flow cytometry (FC).

Target gene	Forward primer (5'-3')	Reverse primer (5'-3')	Probe (Roche Diagnostics)
Actb	aaggccaaccgtgaaaagat	gtggtacgaccagaggcatac	56
Cre	caataccggagatcatgcaa	cactatccaggttacggatatagttca	83
Dll1	aggggagctacacatgttcc	gggctaggagcacactcatc	11
Dll4	tactgctgctggcggtact	gctggttgacgaactcctg	11
Epo	tctgcgacagtcgagttctg	cttctgcacaacccatcgt	16
Hes1	tgccagctgatataatggagaa	ccatgataggctttgatgacttt	83
Hey1	acgacatcgtcccaggttt	actgttattgattcggtctcgtc	72
Hif1a	tgagcttgctcatcagttgc	cataacagaagctttatcaagatgtga	60
Hif2a	tgacagctgacaaggagaaaaa	caactcatagaagacctccgtctc	12
Notch 1	tggacgacaatcagaacgag	cctcaaaccggaacttcttg	85
Notch 4	ccatccagctgatgactcct	atccctgcaccagtgtcct	16
Pecam-1	cggtgttcagcgagatcc	actcgacaggatggaaatcac	45
Vegf (all isoforms)	actggaccctggctttactg	tgggacttctgctctccttc	64

Supplemental Table S4: real-time quantitative PCR primers and probes.

List of primers and probes (Roche Diagnostics, UK) used.

References

Grossman, R., Fox, L. E., Gorovits, R., Ben-Dror, I., Reisfeld, S. and Vardimon, L. (1994). Molecular basis for differential expression of glutamine synthetase in retina glia and neurons. *Mol. Brain Res.* **21**, 312–320.

Hitchcock, P., Macdonald, R., VanDeRyt, J. and Wilson, S. (1996). Antibodies against Pax6 immunostain amacrine and ganglion cells and neuronal progenitors, but not rod precursors, in the normal and regenerating retina of the goldfish. *J Neurobiol* **29**, 399–413.

Jeon, C.-J., Strettoi, E. and Masland, R. H. (1998). The major cell populations of the mouse retina. *J. Neurosci.* **18**, 8936–46.

Koso, H., Minami, C., Tabata, Y., Inoue, M., Sasaki, E., Satoh, S. and Watanabe, S. (2009). CD73, a novel cell surface antigen that characterizes retinal photoreceptor precursor cells. *Investig. Ophthalmol. Vis. Sci.* **50**, 5411–5418.

Liu, H., Kim, S.-Y., Fu, Y., Wu, X., Ng, L., Swaroop, A. and Forrest, D. (2013). An isoform of retinoid-related orphan receptor β directs differentiation of retinal amacrine and horizontal interneurons. *Nat. Commun.* **4**, 1813.

Liyanage, S. E., Fantin, A., Villacampa, P., Lange, C. A., Denti, L., Cristante, E., Smith, A. J., Ali, R. R., Luhmann, U. F., Bainbridge, J. W., et al. (2016). Myeloid-Derived Vascular Endothelial Growth Factor and Hypoxia-Inducible Factor Are Dispensable for Ocular Neovascularization-Brief Report. *Arterioscler. Thromb. Vasc. Biol.* **36**,.

Macosko, E. Z., Basu, A., Satija, R., Nemesh, J., Shekhar, K., Goldman, M., Tirosh, I., Bialas, A. R., Kamitaki, N., Martersteck, E. M., et al. (2015). Highly parallel genome-wide expression profiling of individual cells using nanoliter droplets. *Cell* **161**, 1202–1214.

Ozerdem, U., Grako, K. A., Dahlin-Huppe, K., Monosov, E. and Stallcup, W. B. (2001). NG2 proteoglycan is expressed exclusively by mural cells during vascular morphogenesis. *Dev. Dyn.* **222**, 218–227.

Ruether, K., Feigenspan, A., Pirngruber, J., Leitges, M., Baehr, W. and Strauss, O. (2010). Pkc-a is essential for the proper activation and termination of rod bipolar cell response. *Investig. Ophthalmol. Vis. Sci.* **51**, 6051–6058.

Stanescu-Segall, D., Birke, K., Wenzel, A., Grimm, C., Orgul, S., Fischer, J. A., Born, W. and Hafezi, F. (2015). PAX6 Expression and Retinal Cell Death in a Transgenic Mouse Model for Acute Angle-Closure Glaucoma. *J. Glaucoma* **24**, 426–32.

Tao, C. and Zhang, X. (2014). Development of astrocytes in the vertebrate eye. *Dev. Dyn.* **243**, 1501–1510.